Cell Communication and Signaling

RESEARCH Open Access

TMEM132A regulates Wnt/β-catenin signaling through stabilizing LRP6 during mouse embryonic development

Shin Ae Oh[1,2†], Jiyeon Jeon[1,2†], Su-yeon Je[1,2†], Seoyoung Kim[1,2], Joohyun Jung[1] and Hyuk Wan Ko[1*]

Abstract
The Wnt/β-catenin signaling pathway is crucial for embryonic development and adult tissue homeostasis. Dysregulation of Wnt signaling is linked to various developmental anomalies and diseases, notably cancer. Although numerous regulators of the Wnt signaling pathway have been identified, their precise function during mouse embryo development remains unclear. Here, we revealed that TMEM132A is a crucial regulator of canonical Wnt/β-catenin signaling in mouse development. Mouse embryos lacking Tmem132a displayed a range of malformations, including open spina bifida, caudal truncation, syndactyly, and renal defects, similar to the phenotypes of Wnt/β-catenin mutants. Tmem132a knockdown in cultured cells suppressed canonical Wnt/β-catenin signaling. In developing mice, loss of Tmem132a also led to diminished Wnt/β-catenin signaling. Mechanistically, we showed that TMEM132A interacts with the Wnt co-receptor LRP6, thereby stabilizing it and preventing its lysosomal degradation. These findings shed light on a novel role for TMEM132A in regulating LRP6 stability and canonical Wnt/β-catenin signaling during mouse embryo development. This study provides valuable insights into the molecular intricacies of the Wnt signaling pathway. Further research may deepen our understanding of Wnt pathway regulation and offer its potential therapeutic applications.

Keywords TMEM132A, Wnt/β-catenin signaling, LRP6, Mouse development, Lysosomal degradation

Introduction

The highly conserved Wnt signaling pathway plays a crucial role in embryonic development, tissue homeostasis and cancer. The Wnt signaling pathway has been shown to play vital roles in patterning of the body axis in early embryonic stages [1]. The body axis is patterned through two distinct pathways. Canonical Wnt signaling induces the expression of target genes responsible for neural tube closure and craniofacial development [2, 3], and the non-canonical signaling pathway regulates body axis elongation through a process called convergent extension [4, 5]. Additionally, Wnt signaling is instrumental for limb bud initiation, outgrowth and patterning [6]. Beyond these early roles in defining the body axis, Wnt signaling has also been implicated in the morphogenesis of numerous organs, including the skin, lungs, kidneys and intestine [7–10]. Thus, aberrant activation or inactivation of the Wnt signaling pathway may cause various developmental anomalies, such as neural tube defects, limb deformities, hypoplastic and cystic kidneys, and lung hypoplasia [11].

†Shin Ae Oh, Jiyeon Jeon and Su-yeon Je contributed equally to this work.

*Correspondence:
Hyuk Wan Ko
kohw@yonsei.ac.kr
[1]Department of Biochemistry, College of Life Science and Biotechnology, Yonsei University, Seoul 03722, Korea
[2]Brain Korea 21 (BK21) FOUR Program, Yonsei Education & Research Center for Biosystems, Yonsei University, Seoul 03722, Korea

The Wnt signaling pathway is broadly divided into canonical and noncanonical Wnt signaling pathways. In humans, 19 Wnt ligands bind to a repertoire of 10 Frizzled (FZD) cell-surface receptors and co-receptors, including low-density lipoprotein receptor-related protein 5 and 6 (LRP5/6), retinoic acid receptor-related orphan receptor (ROR), and receptor-like tyrosine kinase (RYK), triggering functionally diverse downstream signaling cascades. In the β-catenin-dependent canonical pathway, Wnt ligands bind to FZD-LRP5/6 heterodimers, leading to the disassembly of the β-catenin destruction complex formed by Axin, casein kinase 1 (CK1), adenomatous polyposis coli (APC) and glycogen synthase kinase-3β (GSK3β) [12]. Liberated β-catenin accumulates in the cytosol and enters the nucleus to co-activate target gene expression with the TCF/LEF (T-cell factor/lymphoid enhancer factor) transcription factor, influencing cell proliferation and differentiation [12]. Conversely, non-canonical Wnt signaling pathways, including the Wnt/planar cell polarity (PCP) pathway and Wnt/Ca^{2+} pathway, operate independently of β-catenin and transduce signals via Rho and Rac small GTPases to regulate cell polarity and movement or via heterotrimeric G proteins to modulate Ca^{2+} signaling [13]. The intricate nature of this pathway arises from the specific combinations of ligands, receptors, and co-receptors, which determine distinct Wnt-based signaling pathways. Although the mechanisms by which cells interpret different Wnt stimuli remain incompletely understood, the presence of co-receptor appears to play a crucial role in determining signaling specificity. For instance, LRP5/6 is essential for the initiation of Wnt/β-catenin signaling, whereas the ROR and RYK co-receptors mediate Wnt/PCP signaling [14–16]. Elucidating the precise nature of Wnt ligand–receptor interactions and their impact on development requires further investigation into co-receptor regulation and the potential discovery of novel co-receptors.

Transmembrane proteins (TMEMs) are known to mediate the signal transduction of various signaling pathways [17]. Among them, a novel single-pass type I transmembrane protein called transmembrane protein 132 A (TMEM132A) has been reported to participate in the Wnt signaling pathway in cultured cells [18]. TMEM132A belongs to the TMEM132 protein family, which consists of five members, TMEM132A-E. The members of this protein family share a common molecular architecture characterized by three tandem immunoglobulin domains and a cohesin domain homolog [19]. Among them, studies have reported the associations of TMEM132D, TMEM132E, and TMEM132B with neurological disorders, while the functions of TMEM132A and TMEM132C are relatively unknown [20–22]. Recent studies have demonstrated that TMEM132A regulates the Wnt signaling pathway by modulating the secretion of Wnt ligands in cultured cells [18]. Furthermore, TMEM132A has been implicated in planar cell polarity (PCP) signaling, where it contributes to neural tube closure and hindgut extension during embryonic development [23]. In contrast, TMEM132A has also been linked to mesoderm migration through the activation of integrin signaling, particularly affecting neural tube closure [24]. Despite these insights, the precise in vivo role of TMEM132A in mouse development, as well as its specific contributions to both canonical and non-canonical Wnt signaling pathways, remains incompletely understood.

Here, we demonstrated that TMEM132A plays a crucial role in canonical Wnt signaling, a pathway essential for embryonic development. Analysis of *Tmem132a* mutant mouse embryos revealed phenotypic hallmarks of disrupted Wnt signaling, including neural tube and limb defects. Mechanistically, TMEM132A physically interacts with the Wnt co-receptor LRP6, and its downregulation destabilizes LRP6, leading to diminished Wnt signaling even in the presence of Wnt ligands. Collectively, our findings identify TMEM132A as a novel regulator of the canonical Wnt/LRP6/β-catenin signaling pathway, highlighting its potential significance in developmental processes and associated pathologies.

Methods

Animals

Tmem132a^{tm1a} mice were bred on a C57BL/6 N background at the Yonsei University's animal facility. All animal procedures were approved by the Yonsei University Institutional Animal Care and Use Committee (IACUC), including housing and breeding protocols. The maternal mice were euthanized at approximately midday following the identification of a vaginal plug, which was designated embryonic day 0.5 (E0.5). The mice were housed in a specific-pathogen-free (SPF) facility at Yonsei University.

Cell culture and transfection

In vitro experiments utilized HEK293, STF-HEK293, and primary mouse embryonic fibroblasts (MEFs) cells. The HEK293 and STF-HEK293 cell lines were obtained from the Korean Cell Bank (KCB) and kindly provided by Dr. Kang-Yell Choi. The primary MEFs were derived from E13.5 embryos obtained by mating *Tmem132a*$^{tm1a/+}$ heterozygous mice. Cells were cultured in Dulbecco's Modified Eagle Medium (DMEM, HyClone) supplemented with 10% fetal bovine serum (FBS, HyClone) and 100 U/mL penicillin (HyClone) at 37°C in a 5% CO_2. Wnt/β-catenin signaling was activated by treating cells with either control medium or Wnt3a-conditioned media from L cells that were genetically engineered to express Wnt3a. HEK293 cells were transiently transfected with either a negative control siRNA (Invitrogen) or a human TMEM132A-targeting siRNA (sequence 5'-AGU CAC

AGC CGC UUC CAC UGA AAC G-3', invitrogen) using Lipofectamine RNAiMAX (Invitrogen) for 30 h. The pCS2-LRP6-EGFP and pCS2-VSVG-LRP6 plasmids were obtained from Dr. Eek-hoon Jho, were co-transfected with siRNAs using Lipofectamine 3000 (Invitrogen) following the manufacturer's instructions.

Luciferase assay

Luciferase assays were performed with STF-HEK293 cells seeded in 24-well culture plates (SPL) at 8×10^4 cells per well. Cells were co-transfected with pRL-TK reporter plasmid (internal control) or indicated plasmids with TMEM132A-siRNA using Lipofectamine 3000. Twenty-four hours post-transfection, cells were treated with Wnt3a-containing media or control media as needed and then harvested in passive lysis buffer (Promega). Luciferase activity was measured using the Promega Dual-Luciferase Reporter Assay Reagent and a GloMax® Discover Microplate Reader (Promega) in 96-well plates.

Immunocytochemistry and confocal microscopy

Cells were seeded at 3×10^4 cells per well on coverslips in 24-well plates and transfected with expression plasmids for cellular localization analysis. Following transfection, cells were fixed with 4% paraformaldehyde (PFA) for 15 min at room temperature and washed with Dulbecco's phosphate-buffered saline (DPBS, HyClone). Fixed cells were permeabilized with wash buffer (1% horse serum (Gibco) and 0.1% Triton X-100 in PBS), then stained with mouse anti-V5 antibodies (Invitrogen) or anti-LRP6 antibodies (Abcam) diluted in wash buffer overnight at 4°C. Cells were washed and incubated with appropriate secondary antibodies and DAPI for 3 h at 4°C. Images were taken on a Zeiss LSM 900 confocal microscope and analyzed using Zeiss Zen software.

Immunoblotting and immunoprecipitation

Embryonic tissues and cells were lysed in RIPA buffer (50 mM Tris·HCl (pH 7.4), 150 mM NaCl, 1 mM EDTA, 1% Nonidet P-40, 0.25% Na-deoxycholate, 0.1% SDS) supplemented with 1 mM PMSF, 1X protease inhibitor and/or phosphatase inhibitor cocktail (Roche). Lysates were clarified by centrifugation at 14,000 rpm for 15 min at 4 °C. The protein concentration was determined by the Bradford assay (Pierce). Proteins were separated by SDS-PAGE and transferred to PVDF membranes (Millipore). Membranes were blocked and then incubated with primary antibodies overnight at 4 °C. After washing, membranes were incubated with appropriate HRP-labeled secondary antibodies for 2 h at 4 °C. Signals were visualized using chemiluminescent reagent (Millipore) and quantified by ImageJ program.

Whole-cell lysates were incubated with specific antibodies overnight at 4 °C and antibody- protein complexes were captured using Dynabeads™ Protein G beads (Invitrogen). Bound proteins were eluted and analyzed by western blotting as described above. The following primary antibodies were used for western blotting: anti-β-catenin (Santa Cruz), anti-active-β-catenin (Millipore), anti-LRP6 (Abcam), α-tubulin (Sigma), β-actin (Santa Cruz), anti-VSVG tag (GenScript), and anti-V5 (Invitrogen).

RNA extraction and quantitative RT–PCR

Total RNA was isolated from cells and E10.5 embryos using TRIzol reagent (Qiagen). One microgram of RNA was reverse transcribed into cDNA using a commercially available First-Strand cDNA Synthesis Kit (Takara). Quantitative RT-PCR (qRT−PCR) was performed using a real-time PCR instrument with with SYBR Premix Ex Taq™ (Takara). The following specific primers were used in this study to quantify target genes: Tmem132a, TGG T CAATGGTGTGGTCTTC (forward) and TCAGTTCCT CCTGGTCAGT (reverse); Axin2 GAT GTC TGG CAG TGG ATG TTA G (forward) and GAC TCC AAT GGG TAG CTC TTT C (reverse); T(brachyury) GCC TAC CAG AAT GAG ATT AC (forward) and CCG GTT CCT CCA TTA CAT CTT (reverse); Tbx6 GCT CCA TCT GTA CCA TCC TTT G (forward) and CTT GGA TCC CAT GTC CAG ATA AC (reverse). Ctnb1 GTA GAG ACA GCT CGT TGT ACT G (forward) and GGG ATG CCA CCA GAC TTA AA (reverse); FZD4 CCT GTG TGA TTG CCT GTT ATT TC (forward) and CAA CTG CCA TGT TTG AGT CAT C (reverse); Lef1 GCA TCC CTC ATC CAG CTA TT (forward) and CTC CTG CTC CTT TCT CTG TTC (reverse). The expression levels of the genes were normalized to those of GAPDH, and the sequences of primers used in this study were as follows: GAPDH, AACAGCAACTCCCACTCTTC (forward), and CCTGTTGCTGTAGCCGTATT (reverse). Relative mRNA levels were calculated using the $2^{-\Delta\Delta Ct}$ method of QuantStudio Design and Analysis software.

Tissue preparation and histology

The organs of mouse embryos were dissected from mouse embryos at indicated time points and fixed in 4% PFA overnight. Paraffin-embedded tissue were sectioned at 4- or 5-μm thickness and stained with hematoxylin and eosin (H&E) for histological analysis.

Quantification and statistical analysis

qRT–PCR and western blot data were normalized to control samples. Normalization was done by dividing the raw data for each sample by the average value of the control. All data are presented as means with standard errors (SEM). Statistical analysis was performed using GraphPad Prism version 8 (GraphPad Software) and are described in figure legends, including the specific

test used. When there was one variable among multiple groups, one-way ANOVA was used, and when comparing two groups, student's t-test was used to perform statistical comparisons between groups, which was appropriate for the specific experimental design. Statistical significance is indicated in the figures and their legends with asterisks (*$P<0.05$; **$P<0.01$; ***$P<0.001$). The specific number of replicates (n) used for each experiment is also provided in the legends.

Results

Loss of TMEM132A disrupts multiple developmental processes in mouse embryos

While investigating novel transmembrane proteins crucial for mouse development, we focused on previously identified embryonic lethal genes from a high-throughput embryonic phenotyping screen [25]. Notably, *Tmem132a* mutant mouse embryos displayed abnormal neural tube and limb development. To further explore the role of TMEM132A during mouse development, we used C57BL6N mice harboring the *Tmem132a*$^{tm1a\ (KOMP)Wtsi}$ allele (*Tmem132a*^{tm1a}), which disrupts TMEM132A function by introducing a splicing acceptor and a reporter gene between exons 1 and 2, resulting in a truncated, nonfunctional transcript of Tmem132a (Supplementary Fig. S1). Homozygous *Tmem132a*$^{tm1a/tm1a}$ embryos died at birth, leading us to analyze various developmental stages to characterize the phenotypic abnormalities. We examined a total of 11 *Tmem132a* mutant embryos and observed a range of developmental defects with varying penetrance and expressivity. All *Tmem132a* mutant pups collected immediately after birth were non-viable, exhibiting no signs of normal breathing or sustained life, supporting the conclusion that *Tmem132a* mutant embryos fail to survive postnatally. By embryonic day 10.5 (E10.5), control embryos displayed fully elongated and closed neural tubes, whereas *Tmem132a*$^{tm1a/tm1a}$ embryos consistently exhibited open and shortened posterior neural tubes (Fig. 1A), which progressed to spina bifida at E13.5 and truncation of the axial skeleton by E18.5 (Fig. 1B). Spina bifida was observed in all 11 mutant embryos, indicating full penetrance for this phenotype.

In addition to spina bifida, we observed other notable developmental defects. Forelimb syndactyly was present in 9 out of 11 mutant embryos (82%), and underdeveloped hindlimb buds were also apparent (Fig. 1C). Examination of organ development at E18.5 revealed that 10 out of 11 mutant embryos (91%) exhibited hypoplastic kidneys, many of which displayed hydronephrosis, characterized by renal pelvis dilation (Fig. 1D). Hypoplastic lungs with restricted alveolar formation were detected in 8 out of 10 mutant embryos (80%) (Fig. 1E), and shortened colons with reduced crypt formation were observed in 10 out of 11 mutant embryos (91%) (Fig. 1F). None of these defects were observed in heterozygous or wild-type embryos. Remarkably, these multiple developmental defects, particularly spina bifida, syndactyly, and renal anomalies, resemble those observed in mouse embryos with dysfunctional Wnt/β-catenin signaling [2, 26–29]. Based on these findings, TMEM132A might be associated with the Wnt signaling pathway during development.

TMEM132A is essential for Wnt/β-catenin signaling activation in developing mouse embryos

Phenotypic analysis of mouse embryos suggested a link between TMEM132A and Wnt signaling. To examine the effect of TMEM132A on Wnt/β-catenin signaling activity in mammalian cells, we transiently knocked down TMEM132A using siRNA in human embryonic kidney (HEK293) cells (Fig. 2A). Subsequently, the cells were treated with Wnt3a-conditioned media (Wnt3a-CM) to activate canonical Wnt signaling. Western blot analysis revealed decreased total and active β-catenin levels in TMEM132A knockdown (KD) cells, indicating reduced Wnt signaling activity (Fig. 2B). We also used HEK293 cells with a stably integrated Super8x TopFlash reporter (STF cells) to measure Wnt/β-catenin transcriptional activity via a luciferase assay [30]. Consistent with these findings, TMEM132A-KD cells exhibited significantly suppressed Wnt signaling upon Wnt ligand treatment (Fig. 2C). Notably, KD cells even exhibited lower basal Wnt activity. To further corroborate the correlation between TMEM132A and the Wnt signaling pathway, we examined whether increased TMEM132A levels enhance Wnt activity. The overexpression of TMEM132A in TMEM132A-KD STF cells reversed the decrease in Wnt signaling (Fig. 2D). Moreover, luciferase assays demonstrated a dose-dependent increase in STF reporter activity with increasing TMEM132A expression (Fig. 2E). These findings collectively demonstrated that TMEM132A positively regulates Wnt/β-catenin signaling in cultured cells.

To validate the regulatory role of TMEM132A in developing mouse embryos, we conducted quantitative reverse transcription PCR (qRT–PCR) on total mRNA extracted from E10.5 wildtype and mutant embryos (Fig. 2F). Mutant embryos displayed significantly reduced expression of Axin2, a well-established direct transcriptional target of the Wnt/β-catenin pathway. Additionally, the mRNA levels of T (Brachyury) and Tbx6, downstream targets of canonical Wnt signaling in the tail bud, were significantly lower in the mutants compared to wild-types (Fig. 2F). Consistent with these findings, Western blot analysis of whole E10.5 embryo lysates revealed decreased levels of both total and active β-catenin protein in mutants compared to controls (Fig. 2G), further corroborating the suppression of Wnt signaling. To

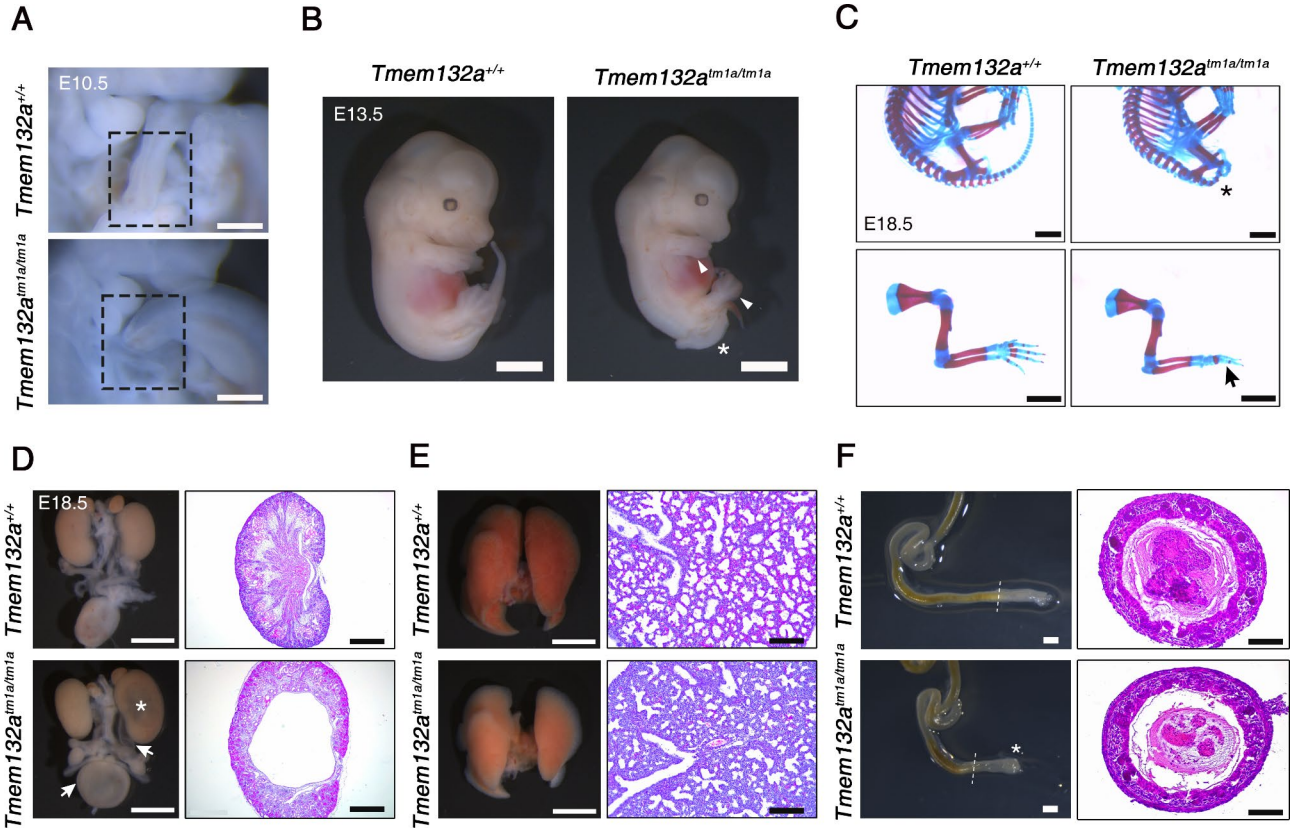

Fig. 1 TMEM132A is crucial for mouse embryonic development. **A**. Abnormal formation of posterior neural tube in *Tmem132a*$^{tm1a/tm1a}$ mice at embryonic day 10.5 (E10.5). The dashed box indicates incomplete elongation and disclosure of the caudal neural tube. Scale bars: 2 mm. **B**. Morphological features of E13.5 mutant mouse embryos. The mutants displayed restrained overall posterior development, characterized by spina bifida (asterisk) and underdeveloped fore and hind limb buds (arrowheads). Scale bars: 2 mm. **C**. Alizarin red/Alcian blue staining of E18.5 embryos revealed truncation of the body axis (asterisk) and forelimb digit loss (arrow) in *Tmem132a*^{tm1a} mutants. Scale bars: 2 mm. **D-F**. Comparison of the morphological and histological features of key organs between E18.5 control and mutant mice. Tissues were fixed in 4% paraformaldehyde overnight, processed for paraffin embedding, and sectioned at 5 µm. (**D**) Loss of TMEM132A caused hydronephrosis, characterized by hypoplastic and/or renal pelvis dilation (asterisk) and a urinary tract filled with fluid (arrows). Hematoxylin and eosin staining of kidney sections provided a detailed view of renal cysts. Scale bars: 2 mm, 200 µm. (**E**) *Tmem132a*^{tm1a} mutants with hypoplastic and less vascularized lungs. Hematoxylin and eosin staining revealed suppressed alveolar formation in the mutants. Scale bars: 2 mm and 200 µm, respectively. (**F**). The mutant mice also exhibited a shortened colon with an obstructed anus (asterisk) but normal histology. The dashed line indicates where the tissue sections were obtained. Scale bars: 2 mm and 100 µm

confirm the effect of TMEM132A deficiency on embryo development, we examined its effect on Wnt signaling in developing organs. qRT−PCR analysis demonstrated reduced expression of Wnt/β-catenin signaling components in E14.5 mutant kidneys and lungs (Fig. 2H, I), demonstrating that TMEM132A is crucial for Wnt signaling activation in multiple developing organs. Together, these results demonstrate that TMEM132A is required for the efficient activation of Wnt signaling both in vitro and in developing mice.

TMEM132A interacts with LRP6 to modulate its stability and potentiate Wnt/β-catenin signaling

Having shown that TMEM132A mediates the Wnt/β-catenin signaling pathway both in vitro and during murine development, we sought to elucidate the underlying mechanism involved. Wnt signaling is activated by the binding of Wnt ligands to frizzled (FZD) receptors and their co receptors, low-density lipoprotein receptor-related proteins (LRPs), primarily LRP5/6 [31]. Interestingly, previous work demonstrated that GRP78, a known TMEM132A binding partner, regulates LRP6 expression by acting as a chaperone [32]. Furthermore, the phenotypic hallmarks of Tmem132a mutant embryos, namely, spina bifida, syndactyly, and renal cysts, strikingly resemble those of LRP6 mutant mice [11, 14, 29]. Collectively, these observations prompted us to hypothesize that TMEM132A modulates Wnt signaling through direct interaction with LRP6.

To test this hypothesis, we first performed immunofluorescence staining of HEK293 and NIH3T3 cells to visualize the subcellular localization of TMEM132A and LRP6. Merged fluorescent signals revealed colocalization in both cell lines (Fig. 3A). Next, co-immunoprecipitation

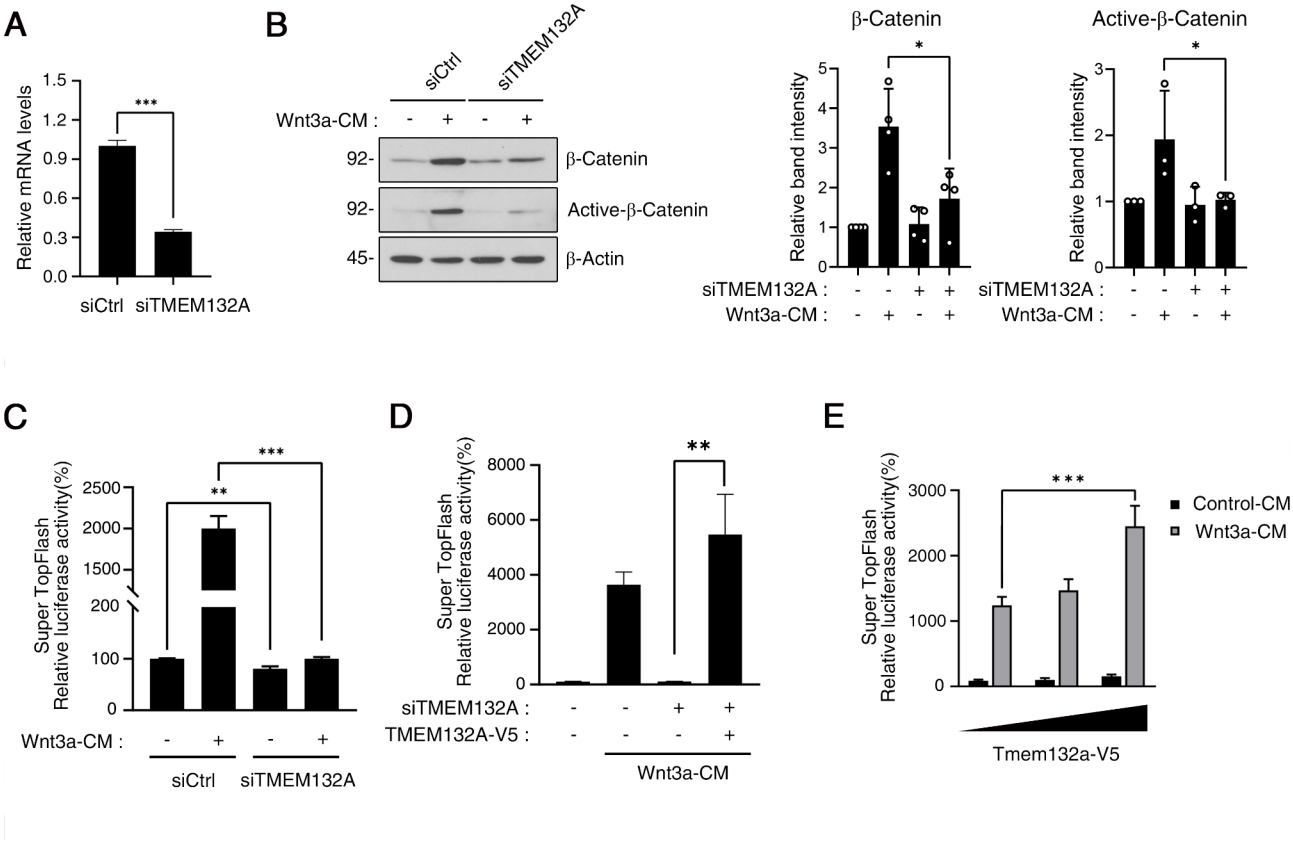

Fig. 2 (See legend on next page.)

(See figure on previous page.)

Fig. 2 TMEM132A regulates Wnt/β-catenin signaling. **A**. qRT–PCR was used to determine the efficiency of TMEM132A knockdown in HEK293 cells. HEK293 cells were transfected with either negative control siRNA or human TMEM132A-siRNA for 30 h and lysed with TRIzol reagent for qRT–PCR. The expression levels of the genes were normalized to that of GAPDH. The data are presented as the mean ± SEM. Statistical significance was determined by two-sided unpaired Student's t tests in GraphPad Prism. ***$P < 0.001$. **B**. TMEM132A-knockdown (KD) and control HEK293 cells were treated with Wnt3a-CM overnight to observe changes in the response to Wnt3a ligands, which was analyzed by western blotting. Knockdown of TMEM132A led to decreased Wnt signaling, as shown by reduced β-catenin and active β-catenin levels. Band intensities were quantified by normalization to β-actin ($n = 3$). The data are presented as the mean ± SEM. Statistical significance was assessed by two-sided unpaired Student's t tests in GraphPad Prism. *$P < 0.05$. **C**. Dual-luciferase assays were used to examine the transcriptional Wnt activity in TMEM132A-KD STF-HEK293 cells. HEK293 cells stably expressing the SuperTopflash reporter were transfected with TMEM132A-siRNA or control siRNA and treated with Wnt3a-CM. The data are presented as the mean ± SEM. Statistical significance was assessed by two-sided unpaired Student's t tests. **$P < 0.01$; ***$P < 0.001$. **D**. Overexpression of TMEM132A rescues inhibited Wnt signaling in TMEM132A-KD cells. STF-HEK293 cells were transfected with siRNA and/or the TMEM132A-V5 expression vector along with Renilla vectors. The data are presented as the mean ± SEM ($n = 3$). Statistical significance was assessed by two-sided unpaired Student's t tests in GraphPad Prism. **$P < 0.01$. **E**. TMEM132A overexpression increases Wnt signaling activity in a dose-dependent manner in STF-HEK cells. The data are presented as the mean ± SEM. Statistical significance was assessed by Tukey's multiple comparisons test in GraphPad Prism. *$P < 0.05$. **F**. mRNA expression analysis of downstream Wnt/β-catenin target genes in control and *Tmem132A*^{tm1a} mutant mouse embryos at E10.5 revealed decreased Wnt signaling activity in mutants. Total RNA was extracted from whole mouse embryos and analyzed by qRT-PCR ($n = 5$). The expression levels of the genes were normalized to GAPDH. Data are presented as the mean ± SEM. Statistical significance was assessed by two-sided unpaired Student's t tests. *$P < 0.05$; **$P < 0.01$; and ***$P < 0.001$. **G**. Western blotting analysis of protein lysates from whole E10.5 embryos showed reduced Wnt signaling in mutants. Band intensities were normalized to β-actin ($n = 4$). Data are presented as the mean ± SEM. Statistical significance was assessed by two-sided unpaired Student's t tests. **$P < 0.01$. **H**, **I**. Decreased expression of Wnt/β-catenin signaling components in organs of E14.5 *Tmem132a* mutant mice. qRT-PCR analysis of E14.5 lungs (H) and kidneys (I) revealed downregulation of Wnt/β-catenin signaling comonents in *Tmem132a* mutant organs compared to controls. Total RNA was extracted and analysed by qRT–PCR. The expression levels of the genes were normalized to GAPDH. Data are presented as the mean ± SEM. Statistical significance was determined by Dunnett's multiple comparisons test. *$P < 0.05$; **$P < 0.01$; and ***$P < 0.001$

experiments using V5-tagged TMEM132A and VSVG-LRP6 confirmed their interaction at the protein level (Fig. 3B). We further examined whether TMEM132A KD affects the LRP6 protein level. Western blot analysis demonstrated a marked decrease in the level of the LRP6 protein in the TMEM132A-KD cells after Wnt3a stimulation compared to the control cells (Fig. 3C). To validate these results in a genetically engineered system, *Tmem132a* mutant MEFs treated with Wnt3a for 24 h exhibited decreased levels of the LRP6 and β-catenin proteins, indicating impaired Wnt signaling (Fig. 3D). Similarly, compared with wild-type embryos, E10.5 mutant embryos exhibited suppressed LRP6 and β-catenin protein expression (Fig. 3E). In addition, immunofluorescence analysis in *Tmem132a* mutant MEFs, as shown in Supplementary Fig. 2, revealed a reduction in LRP6 protein levels under both untreated and Wnt3a-CM treated conditions. These in vivo findings support the notion that TMEM132A regulates Wnt signaling by influencing LRP6 stability.

TMEM132A stabilizes LRP6 through the inhibition of lysosomal degradation

To elucidate the mechanism by which TMEM132A regulates LRP6 stability, we further examined LRP6 protein turnover using cycloheximide (CHX), a protein synthesis inhibitor. in TMEM132A-KD cells. Cells depleted of TMEM132A via siRNA transfection were treated with CHX for 6 h. Compared to control siRNA-treated cells, TMEM132A KD cells displayed a significantly faster decrease in LRP6 protein levels (Fig. 4A). This indicates that TMEM132A deficiency destabilizes LRP6.

Given the known roles of the ubiquitin–proteasome system and lysosomes in LRP6 degradation, we utilized MG132, a proteasome inhibitor, and bafilomycin-A1, a lysosomal proton pump inhibitor, to dissect the underlying pathway involved. MG132 treatment did not affect LRP6 degradation in TMEM132A-knockdown cells, whereas bafilomycin A1 treatment prevented LRP6 degradation (Fig. 4B, C). These findings demonstrate that TMEM132A specifically stabilizes LRP6 by inhibiting lysosomal degradation.

Discussion

The Wnt signaling pathway is a fundamental regulator of embryonic development and tissue homeostasis, and its dysregulation is implicated in various developmental anomalies and diseases. In this study, we elucidated the pivotal role of TMEM132A, a single-pass transmembrane protein, in regulating the canonical Wnt/β-catenin signaling pathway during mouse embryo development. These findings underscore TMEM132A as a novel regulator that modulates the stability of LRP6, thereby influencing the activation of Wnt signaling.

The role of TMEM132A in early mouse embryo development has been suggested to be important for caudal body patterning. Disruption of Tmem132a in mouse embryos has been shown to markedly cause caudal neural tube closure defects [23, 24]. Studies have concluded that TMEM132A is involved in two distinct pathways that contribute to these defects. First, TMEM132A is implicated in directional mesodermal cell migration, where it controls the protein levels of collagen-binding integrin heterodimers to activate the integrin signaling pathway, a key regulator of cell-matrix interactions required for migration. Additionally, TMEM132A has been linked to planar cell polarity (PCP) signaling, which

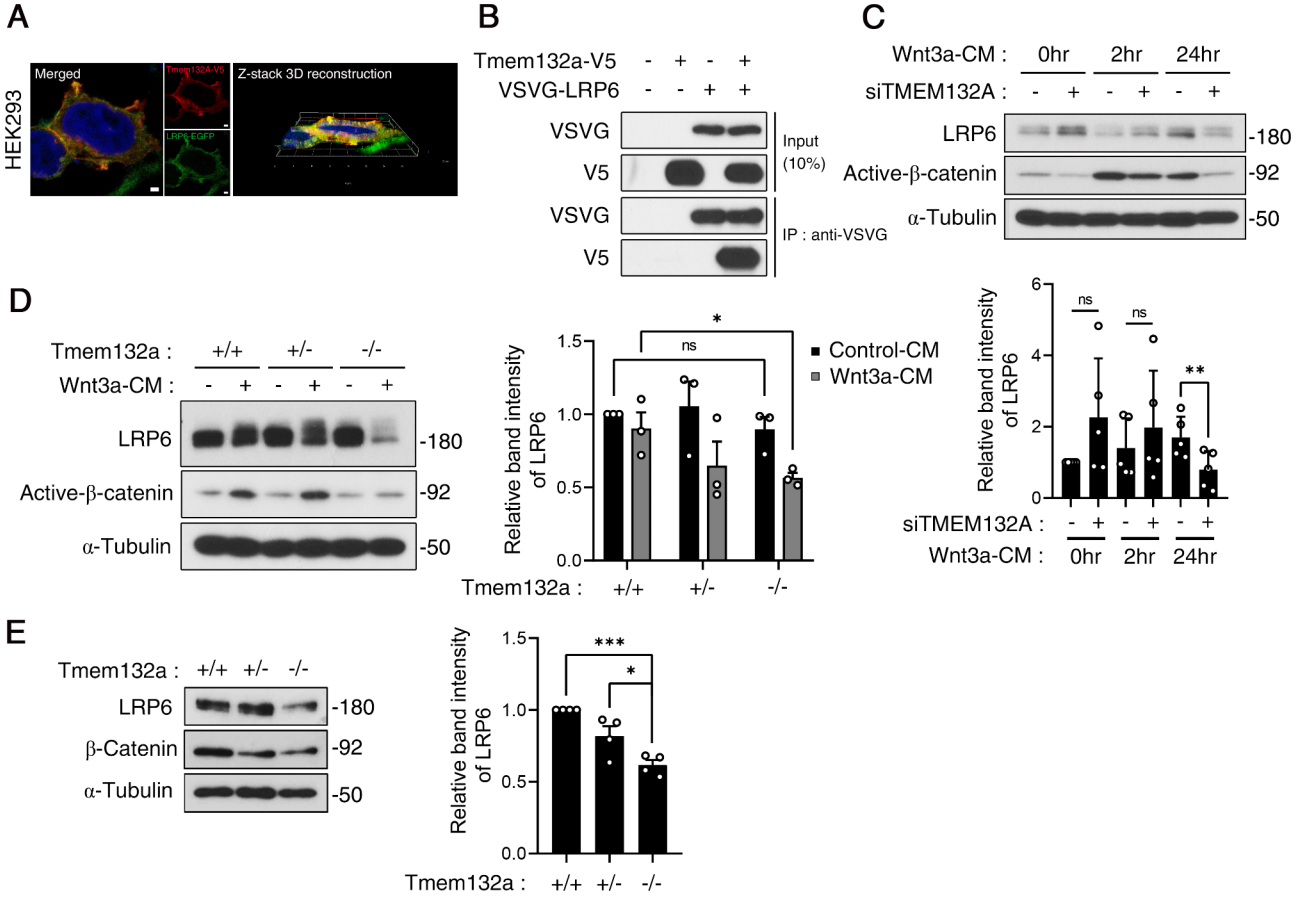

Fig. 3 TMEM132A regulates Wnt/β-catenin signaling through LRP6. **A**. TMEM132A partially co-localized with LRP6, as indicated by the merged signal (yellow). HEK293 cells co-transfected with Tmem132a-V5 and LRP6-EGFP plasmids were immunostained with V5 (red) and imaged by confocal microscopy. Nuclei were stained with DAPI. 3D reconstruction of a confocal z-stack showing colocalization of TMEM132A and LRP6. Scale bar: 2 μm. **B**. Co-IP showing the interaction of TMEM132A with LRP6 in HEK293 cells. TMEM132A-V5 and VSVG-LRP6 were overexpressed in HEK293 cells and pulled down by a VSVG antibody in a co-IP experiment. **C**. Western blot analysis showed decreased protein levels of LRP6 and active β-catenin in TMEM132A-KD cells upon chronic stimulation with Wnt3a. HEK293 cells with TMEM132A-siRNA-mediated knockdown were treated with Wnt3a-CM for the indicated times and harvested for western blot analysis. Total protein levels were analyzed by western blotting, and relative band intensities were normalized to those of α-tubulin. The data are presented as the mean ± SEM ($n = 5$). Statistical significance was assessed by Tukey's multiple comparisons test in GraphPad Prism. $^{**}P < 0.01$. **D**. The protein expression of LRP6 decreased in Wnt3a-treated *Tmem132a* mutant MEFs compared with control MEFs. *Tmem132a* wild-type, heterozygous, and mutant MEFs were treated with Wnt3a-CM overnight and analyzed by western blotting. Total protein levels were analyzed by western blotting, and relative band intensities were normalized to those of α-tubulin. The data are presented as the mean ± SEM ($n = 3$). Statistical significance was assessed by Dunnett's multiple comparisons test in GraphPad Prism. $^{*}P < 0.05$. **E**. The LRP6 protein level decreased in E10.5 *Tmem132a* mutant mouse embryos. Total protein lysate was obtained from E10.5 *Tmem132a*^{tm1a} embryos and analyzed by western blotting. Relative band intensities were normalized to those of α-tubulin. Total protein levels were analyzed by western blotting, and relative band intensities were normalized to those of α-tubulin. The data are presented as the mean ± SEM ($n = 4$). Statistical significance was assessed by Tukey's multiple comparisons test in GraphPad Prism. $^{***}P < 0.001$

is essential for proper neural tube closure and hindgut extension. Both pathways highlight the importance of TMEM132A in coordinating complex signaling mechanisms during embryonic development.

A truncated body axis and an open spina bifida have also been frequently observed in mouse mutants of core Wnt/planar cell polarity (PCP) genes [33]. Additionally, previous studies in *Tmem132a*-null mouse embryos have indicated that TMEM132A disruption leads to multiple defects in caudal body patterning by affecting the non-canonical Wnt/PCP pathway [23]. In contrast, our findings provide evidence that TMEM132A also plays a significant role in regulating the canonical Wnt/β-catenin signaling pathway. However, it is important to note that the involvement of both canonical and non-canonical pathways may contribute to the observed developmental defects in *Tmem132a* mutants, reflecting the complexity of TMEM132A's function during mouse development. For example, LRP6 is a key cell surface receptor for the canonical Wnt/β-catenin signaling pathway, but it also modulates non-canonical pathway [34]. *Lrp6* conditional null embryos exhibit caudal body patterning malformations, which are similar but more severe and broader defects than those observed in *Tmem132a* mutants [27].

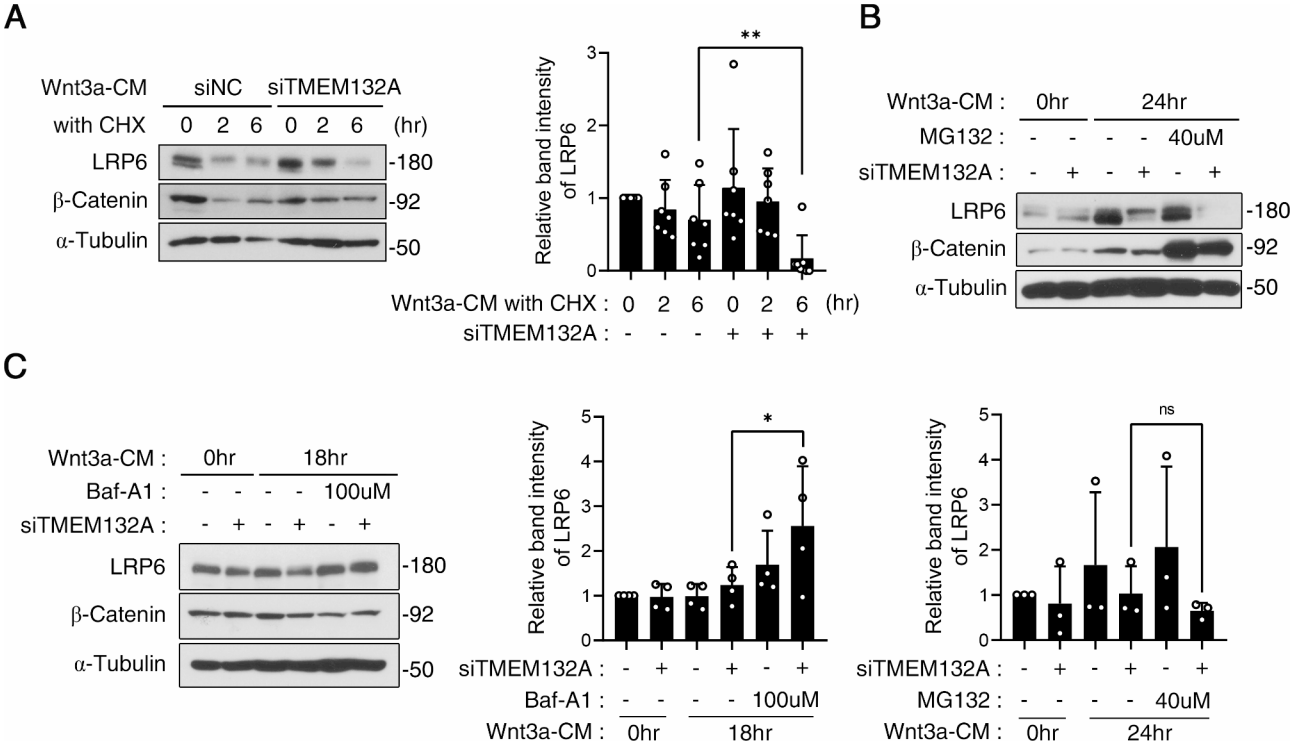

Fig. 4 TMEM132A regulates LRP6 stability by blocking the autophagy degradation pathway. **A**. Western blotting showed decreased protein levels of LRP6 and active β-catenin in TMEM132A-KD cells upon chronic stimulation with Wnt3a. Transfection of HEK293 cells with control or TMEM132A-siRNA was performed, and the cells were treated with cycloheximide (35 μM) in Wnt3a-CM for the indicated times. Total protein levels were analyzed by western blotting, and relative band intensities were normalized to those of α-tubulin. The data are presented as the mean ± SEM ($n = 7$). Statistical significance was assessed by two-sided unpaired Student's t tests in GraphPad Prism. $^{**}P < 0.01$. **B**. Decreased protein levels of LRP6 were observed upon treatment with MG132 (40 μM) ($n = 4$). Total protein levels were analyzed by western blotting, and relative band intensities were normalized to those of α-tubulin. The data are presented as the mean ± SEM. Statistical significance was assessed by two-sided unpaired Student's t tests in GraphPad Prism. **C**. Maintenance of LRP6 protein expression upon treatment with bafilomycin A1 (100 μM). Total protein levels were analyzed by western blotting, and relative band intensities were normalized to those of α-tubulin. The data are presented as the mean ± SEM ($n = 3$). Statistical significance was assessed by Tukey's multiple comparisons test in GraphPad Prism. $^{*}P < 0.05$

Together with our results shown in Fig. 3, these findings might suggest that the multiple defects in *Tmem132a*-null embryos could be caused by disruption of the interaction between TMEM132A and LRP6, leading to both the canonical and non-canonical of Wnt/β-catenin signaling pathways in embryonic development.

Our findings significantly extend the understanding of the role of TMEM132A beyond its previously reported involvement in canonical Wnt/β-catenin signaling by regulating Wnt ligand secretion in cultured cells [18]. The developmental anomalies observed in *Tmem132a* mutant mice provide in vivo evidence of the crucial role of TMEM132A in Wnt-mediated developmental processes. The spectrum of phenotypes, including spina bifida, limb syndactyly, and organ hypoplasia, mirrors the disruptions in Wnt signaling pathways previously associated with these defects. These phenotypic manifestations highlight the critical role of TMEM132A in regulating Wnt/β-catenin signaling during embryogenesis. Furthermore, our findings contribute to deepening the molecular basis of TMEM132A in the Wnt signaling pathway. In vitro studies further support the link between TMEM132A and Wnt signaling, as knockdown of TMEM132A in cultured cells leads to diminished Wnt/β-catenin signaling, whereas overexpression of TMEM132A enhances Wnt signaling. These findings indicate that TMEM132A positively regulates canonical Wnt signaling in mammalian cells. The interaction between TMEM132A and LRP6 represents a critical step in the canonical Wnt signaling cascade. Through co-immunoprecipitation and immunofluorescence experiments, we established that TMEM132A physically interacts with LRP6, suggesting a model in which TMEM132A acts to stabilize LRP6, thus facilitating its role in propagating Wnt signaling. The reduction in LRP6 and β-catenin levels in TMEM132A-deficient cells upon Wnt3a stimulation underscores the importance of TMEM132A in maintaining LRP6 availability for effective Wnt signal transduction. This mechanism is further supported by our observations of accelerated LRP6 degradation via lysosomal pathways in the absence of TMEM132A, highlighting a specific role for TMEM132A in protecting LRP6 from lysosomal

degradation. The demonstration that TMEM132A directly interacts with LRP6 and modulates its stability indicates a pivotal mechanism by which TMEM132A influences canonical Wnt signaling. This interaction suggests that TMEM132A plays a protective role against lysosomal degradation of LRP6, thereby ensuring the sustained presence of this co-receptor at the cell surface to engage in signaling events.

Our study identified TMEM132A as a novel regulator of the canonical Wnt/β-catenin signaling pathway through its interaction with and stabilization of LRP6 during mouse embryo development. These findings not only expand our understanding of Wnt signaling regulation but also provide insights into the molecular basis of developmental disorders associated with dysregulated Wnt signaling. Future studies may explore TMEM132A as a potential therapeutic target for treating various diseases, including congenital anomalies and cancers, associated with aberrant Wnt signaling.

Abbreviations

TMEM132A	Transmembrane proteins 132 A
LRP	Lipoprotein receptor-related protein
FZD	Frizzled
ROR	Retinoic acid receptor-related orphan receptor
RYK	Receptor-like tyrosine kinase
CK1	Casein kinase 1
APC	Adenomatous polyposis coli
GSK3β	Glycogen synthase kinase-3β
TCF/LEF	T-cell factor/lymphoid enhancer factor
Tbx6	T-Box transcription factor 6
Axin2	Axis inhibition protein 2
PCP	Planar cell polarity
GRP78	Glucose-regulated protein 78
VSVG	Vesicular stomatitis virus G
CHX	Cycloheximide

Supplementary Information

The online version contains supplementary material available at https://doi.org/10.1186/s12964-024-01855-9.

Supplementary Material 1

Supplementary Material 2

Acknowledgements

We are very grateful to members of our laboratory for providing valuable and constructive comments on the manuscript. We also thank Dr. Kang-Yell Choi (Yonsei University) for sharing STF-HEK293 cell line, and Dr. Eek-Hoon Jho (University of Seoul) for pCS2-LRP6-EGFP and pCS2-VSVG-LRP6 plasmids.

Author contributions

H.W. Ko led the study design and prepared the manuscript. S.A. Oh, J. Jeon, S. Je, and S. Kim carried out the experiments and wrote the manuscript. J. Jung performed the western blotting analysis. All the authors have read and approved the final manuscript.

Funding

This research was supported by the Basic Science Research Program through National Research Foundation of Korea (NRF) grants funded by the Korea government (MSIT) (NRF-2021R1A2C1012857, NRF-2014M3A9D5A01073969, and NRF-2022M3A9B6082668 to H.W.K.).

Data availability

No datasets were generated or analysed during the current study.

Declarations

Competing interests

The authors declare no competing interests.

Received: 19 March 2024 / Accepted: 27 September 2024
Published online: 09 October 2024

References

1. Miller RK, McCrea PD. Wnt to build a tube: contributions of wnt signaling to epithelial tubulogenesis. Dev Dyn. 2010;239:77–93. https://doi.org/10.1002/dvdy.22059.
2. Zhao T, Gan Q, Stokes A, Lassiter RN, Wang Y, Chan J, Han JX, Pleasure DE, Epstein JA, Zhou CJ. β-catenin regulates Pax3 and Cdx2 for caudal neural tube closure and elongation. Development. 2014;141:148–57. https://doi.org/10.1242/dev.101550.
3. Wang Y, Song L, Zhou CJ. The canonical Wnt/β-catenin signaling pathway regulates Fgf signaling for early facial development. Dev Biol. 2011;349:250–60. https://doi.org/10.1016/j.ydbio.2010.11.004.
4. Ybot-Gonzalez P, Savery D, Gerrelli D, Signore M, Mitchell CE, Faux CH, Greene ND, Copp AJ. Convergent extension, planar-cell-polarity signalling and initiation of mouse neural tube closure. Development. 2007;134:789–99. https://doi.org/10.1242/dev.000380.
5. Wallingford JB. Planar cell polarity, ciliogenesis and neural tube defects. Hum Mol Genet. 2006;15:R227–34. https://doi.org/10.1093/hmg/ddl216.
6. Geetha-Loganathan P, Nimmagadda S, Scaal M. Wnt signaling in limb organogenesis. Organogenesis. 2008;4:109–15. https://doi.org/10.4161/org.4.2.5857.
7. Veltri A, Lang C, Lien WH. Concise Review: wnt signaling pathways in skin development and epidermal stem cells. Stem Cells. 2018;36:22–35. https://doi.org/10.1002/stem.2723.
8. Aros CJ, Pantoja CJ, Gomperts BN. Wnt signaling in lung development, regeneration, and disease progression. Commun Biology. 2021;4:601. https://doi.org/10.1038/s42003-021-02118-w.
9. Meng P, Zhu M, Ling X, Zhou L. Wnt signaling in kidney: the initiator or terminator? J Mol Med (Berl). 2020;98:1511–23. https://doi.org/10.1007/s00109-020-01978-9.
10. Kim BM, Mao J, Taketo MM, Shivdasani RA. Phases of canonical wnt signaling during the development of mouse intestinal epithelium. Gastroenterology. 2007;133:529–38. https://doi.org/10.1053/j.gastro.2007.04.072.
11. Carter M, Chen X, Slowinska B, Minnerath S, Glickstein S, Shi L, Campagne F, Weinstein H, Ross ME. Crooked tail (cd) model of human folate-responsive neural tube defects is mutated in wnt coreceptor lipoprotein receptor-related protein 6. Proc Natl Acad Sci U S A. 2005;102:12843–8. https://doi.org/10.1073/pnas.0501963102.
12. Clevers H, Nusse R. Wnt/β-catenin signaling and disease. Cell. 2012;149:1192–205. https://doi.org/10.1016/j.cell.2012.05.012.
13. Angers S, Moon RT. Proximal events in wnt signal transduction. Nat Rev Mol Cell Biol. 2009;10:468–77. https://doi.org/10.1038/nrm2717.
14. Pinson KI, Brennan J, Monkley S, Avery BJ, Skarnes WC. An LDL-receptor-related protein mediates wnt signalling in mice. Nature. 2000;407:535–8. https://doi.org/10.1038/35035124.
15. Tamai K, Semenov M, Kato Y, Spokony R, Liu C, Katsuyama Y, Hess F, Saint-Jeannet JP, He X. LDL-receptor-related proteins in wnt signal transduction. Nature. 2000;407:530–5. https://doi.org/10.1038/35035117.
16. Yang Y, Mlodzik M. Wnt-Frizzled/planar cell polarity signaling: cellular orientation by facing the wind (wnt). Annu Rev Cell Dev Biol. 2015;31:623–46. https://doi.org/10.1146/annurev-cellbio-100814-125315.
17. Schmit K, Michiels C. TMEM Proteins in Cancer: a review. Front Pharmacol. 2018;9. https://doi.org/10.3389/fphar.2018.01345.
18. Li B, Niswander LA. TMEM132A, a novel wnt signaling pathway Regulator through Wntless (WLS) Interaction. Front Cell Dev Biology. 2020;8. https://doi.org/10.3389/fcell.2020.599890.
19. Sanchez-Pulido L, Ponting CP. TMEM132: an ancient architecture of cohesin and immunoglobulin domains define a new family of neural adhesion

molecules. Bioinformatics. 2018;34:721–4. https://doi.org/10.1093/bioinformatics/btx689.
20. Gregersen NO, Buttenschøn HN, Hedemand A, Dahl HA, Kristensen AS, Clementsen B, Woldbye DP, Koefoed P, Erhardt A, Kruse TA, et al. Are TMEM genes potential candidate genes for panic disorder? Psychiatr Genet. 2014;24:37–41. https://doi.org/10.1097/ypg.0000000000000022.
21. Shifman S, Bronstein M, Sternfeld M, Pisanté-Shalom A, Lev-Lehman E, Weizman A, Reznik I, Spivak B, Grisaru N, Karp L, et al. A highly significant association between a COMT haplotype and schizophrenia. Am J Hum Genet. 2002;71:1296–302. https://doi.org/10.1086/344514.
22. Lane JM, Liang J, Vlasac I, Anderson SG, Bechtold DA, Bowden J, Emsley R, Gill S, Little MA, Luik AI, et al. Genome-wide association analyses of sleep disturbance traits identify new loci and highlight shared genetics with neuropsychiatric and metabolic traits. Nat Genet. 2017;49:274–81. https://doi.org/10.1038/ng.3749.
23. Zeng H, Liu A. TMEM132A regulates mouse hindgut morphogenesis and caudal development. Development. 2023;150:dev201630. https://doi.org/10.1242/dev.201630.
24. Li B, Brusman L, Dahlka J, Niswander LA. TMEM132A ensures mouse caudal neural tube closure and regulates integrin-based mesodermal migration. Development. 2022;149:dev200442. https://doi.org/10.1242/dev.200442.
25. Dickinson ME, Flenniken AM, Ji X, Teboul L, Wong MD, White JK, Meehan TF, Weninger WJ, Westerberg H, Adissu H, et al. High-throughput discovery of novel developmental phenotypes. Nature. 2016;537:508–14. https://doi.org/10.1038/nature19356.
26. Huybrechts Y, Mortier G, Boudin E, Van Hul W. WNT signaling and bone: lessons from skeletal dysplasias and disorders. Front Endocrinol (Lausanne). 2020;11:165. https://doi.org/10.3389/fendo.2020.00165.
27. Zhou CJ, Wang YZ, Yamagami T, Zhao T, Song L, Wang K. Generation of Lrp6 conditional gene-targeting mouse line for modeling and dissecting multiple birth defects/congenital anomalies. Dev Dyn. 2010;239:318–26. https://doi.org/10.1002/dvdy.22054.
28. Karner CM, Chirumamilla R, Aoki S, Igarashi P, Wallingford JB, Carroll TJ. Wnt9b signaling regulates planar cell polarity and kidney tubule morphogenesis. Nat Genet. 2009;41:793–9. https://doi.org/10.1038/ng.400.
29. Wang Y, Stokes A, Duan Z, Hui J, Xu Y, Chen Y, Chen HW, Lam K, Zhou CJ. LDL receptor-related protein 6 modulates Ret Proto-Oncogene Signaling in Renal Development and cystic dysplasia. J Am Soc Nephrol. 2016;27:417–27. https://doi.org/10.1681/asn.2014100998.
30. Coombs GS, Yu J, Canning CA, Veltri CA, Covey TM, Cheong JK, Utomo V, Banerjee N, Zhang ZH, Jadulco RC, et al. WLS-dependent secretion of WNT3A requires Ser209 acylation and vacuolar acidification. J Cell Sci. 2010;123:3357–67. https://doi.org/10.1242/jcs.072132.
31. Zeng X, Huang H, Tamai K, Zhang X, Harada Y, Yokota C, Almeida K, Wang J, Doble B, Woodgett J, et al. Initiation of wnt signaling: control of wnt coreceptor Lrp6 phosphorylation/activation via frizzled, dishevelled and axin functions. Development. 2008;135:367–75. https://doi.org/10.1242/dev.013540.
32. Xiong H, Xiao H, Luo C, Chen L, Liu X, Hu Z, Zou S, Guan J, Yang D, Wang K. GRP78 activates the Wnt/HOXB9 pathway to promote invasion and metastasis of hepatocellular carcinoma by chaperoning LRP6. Exp Cell Res. 2019;383:111493. https://doi.org/10.1016/j.yexcr.2019.07.006.
33. Kibar Z, Vogan KJ, Groulx N, Justice MJ, Underhill DA, Gros P. Ltap, a mammalian homolog of Drosophila Strabismus/Van Gogh, is altered in the mouse neural tube mutant Loop-tail. Nat Genet. 2001;28:251–5. https://doi.org/10.1038/90081.
34. Gray JD, Kholmanskikh S, Castaldo BS, Hansler A, Chung H, Klotz B, Singh S, Brown AM, Ross ME. LRP6 exerts non-canonical effects on wnt signaling during neural tube closure. Hum Mol Genet. 2013;22:4267–81. https://doi.org/10.1093/hmg/ddt277.

Publisher's note